

**Slow earthquakes illuminating interplate coupling heterogeneities in subduction zones**

Satoru Baba<sup>1</sup>, Shunsuke Takemura<sup>1</sup>, Kazushige Obara<sup>1</sup>, and Akemi Noda<sup>2</sup>

1. Earthquake Research Institute, The University of Tokyo
2. National Research Institute for Earth Science and Disaster Resilience

**Contents of this file**

Text S1  
Figures S1 to S6

**Additional Supporting Information (Files uploaded separately)**

Data Set S1

**Introduction**

This supporting information file includes one supplemental text and six supplemental figures. Text S1 describes the error of the cumulative moment of each grid. Figure S1 presents the virtual epicentral grids analysed in this study. Figure S2 presents the frequency distribution of VLFES. Figure S3 presents the distribution of the number of detected events in each virtual epicentral grid. Figure S4 presents the cumulative numbers of events detected from January 2003 to June 2019. Figure S5 presents the temporal variation of the moment density release rate. Figure S6 presents the relationship between the moment density release rate after huge earthquakes and interplate coupling rate.

Additional Supporting Information includes the detected VLFE catalog (Data Set S1).

## Text S1.

### Error estimation

We evaluated the errors of the cumulative moment of each grid by using the nonparametric bootstrap method (Tichelaar & Ruff, 1989). First, 500 bootstrap samples were prepared for each grid. A bootstrap sample was generated from the original events. If  $n$  events were detected in a grid, a bootstrap sample consisted of  $n$  events including duplicates. Subsequently, cumulative moments were calculated by the sum of the moments of  $n$  events. Finally, we estimated the standard deviations of the 500 cumulative moments.

We also estimated the errors of the cross-correlation coefficients between the moment density release rate and the coupling ratio using the nonparametric bootstrap method. The 500 bootstrap samples, which were generated from the 49 original grids, were prepared and a bootstrap sample consisted of 49 grids including duplicates. Cross-correlation coefficients were calculated for each bootstrap sample. We then estimated the standard deviations of the 500 cross-correlation coefficients.

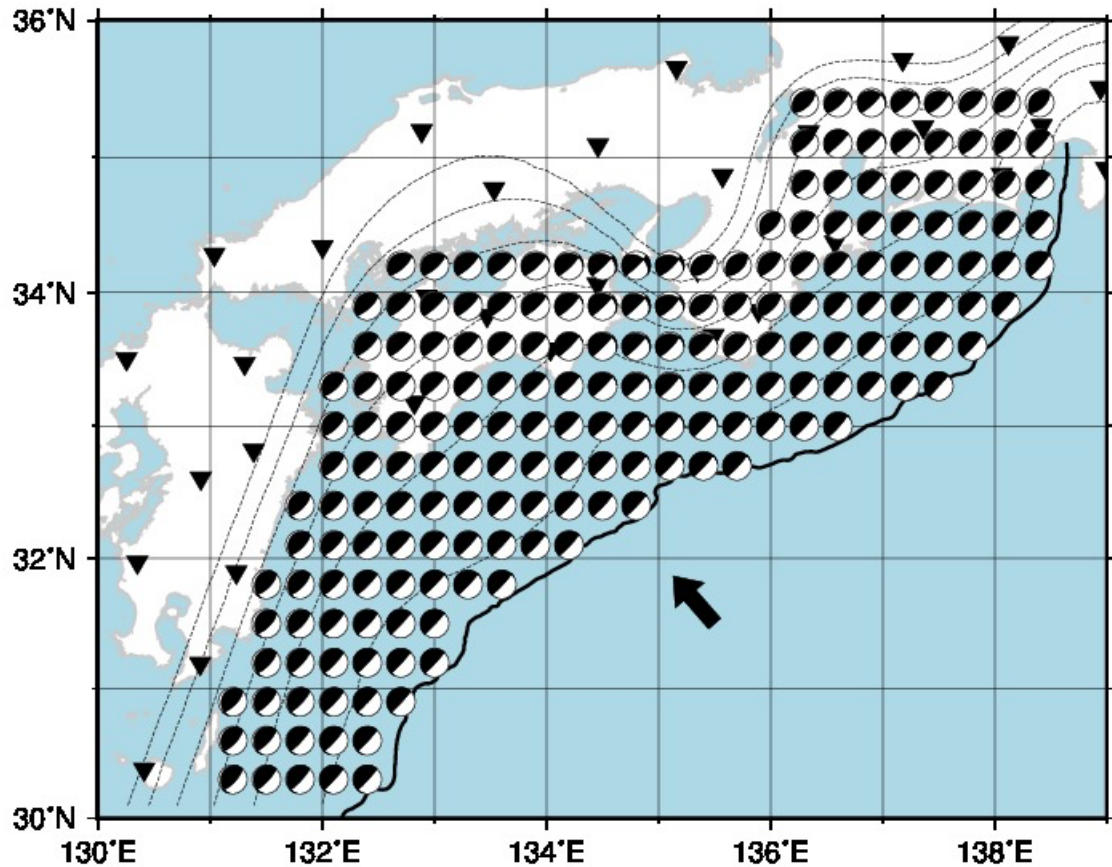


**Figure S1.** Virtual epicentral grids analysed in this study. Beach balls indicate the places and focal mechanisms of virtual sources. Inverted triangles represent the F-net station locations used in this study. The black line, black arrows, and dashed contours are the same as those in Figure 1.

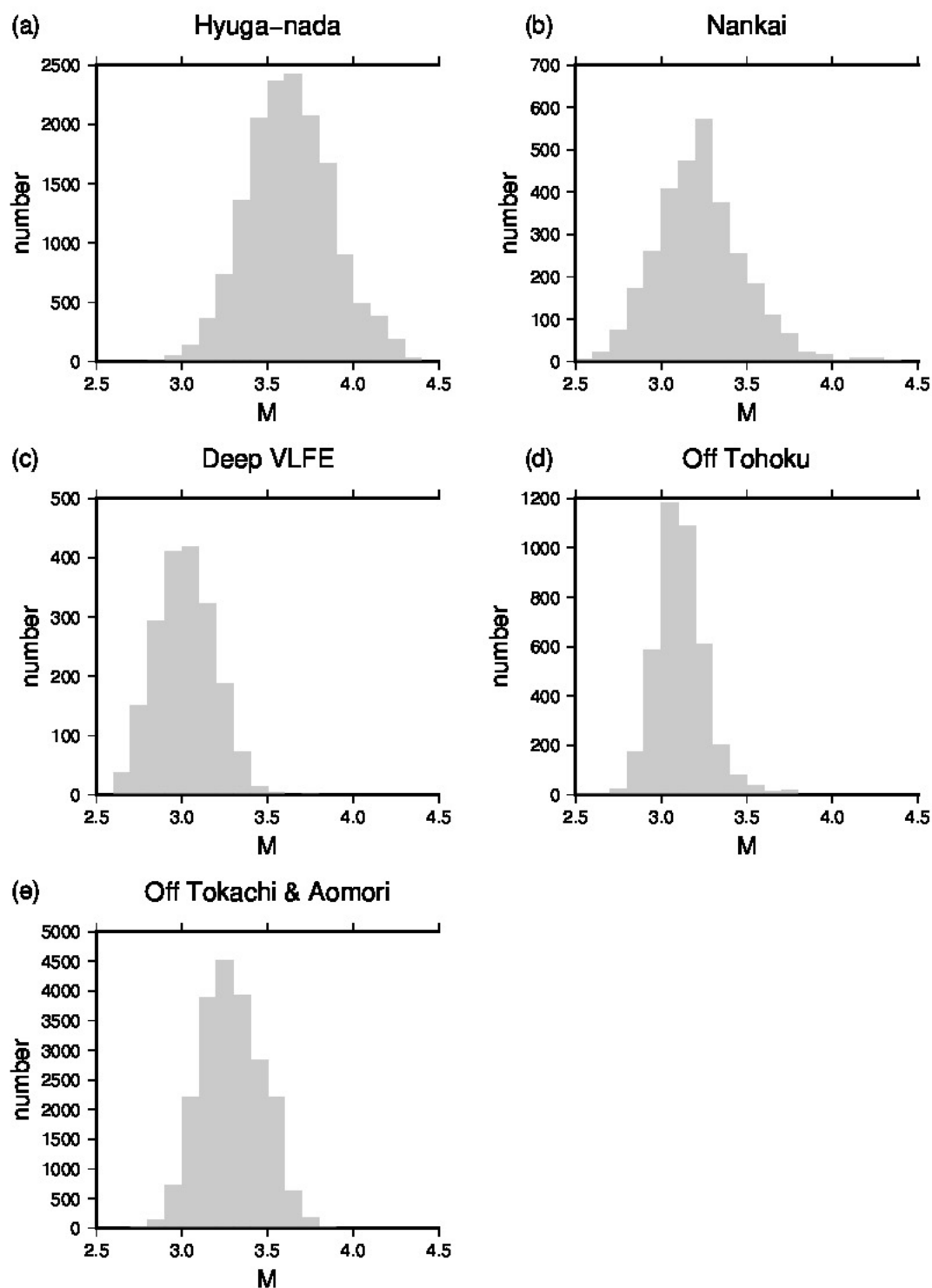


**Figure S2.** Frequency distribution of VLFs. (a) Shallow VLFs in Hyuga-nada, (b) Shallow VLFs in Nankai, except for Hyuga-nada, (c) Deep VLFs along the Nankai Trough, (d) Off Tohoku region, and (e) Off Tokachi and off Aomori.

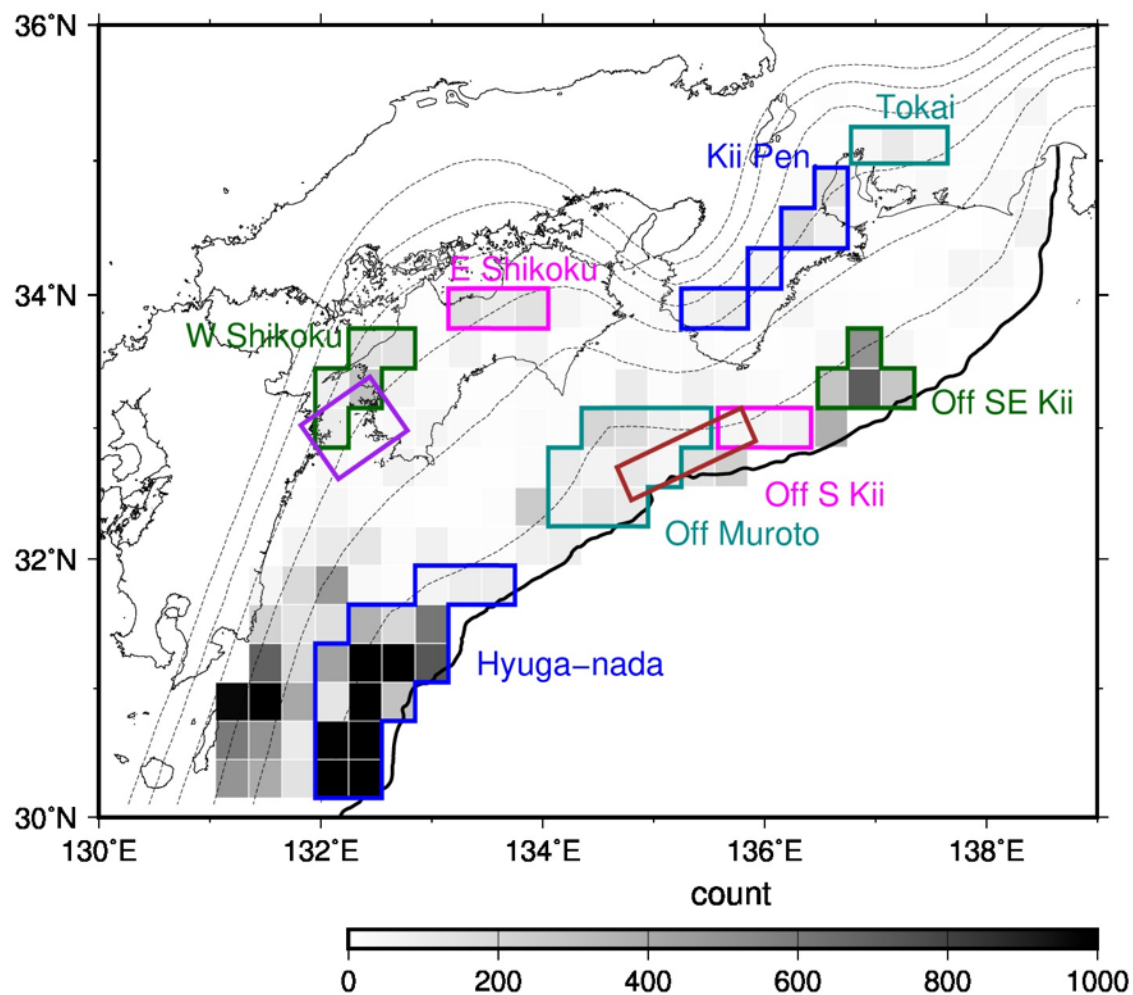


**Figure S3.** Distribution of the number of detected events in each virtual epicentral grid. The black line, dashed contours, and purple and brown rectangles are the same as those in Figure 1.

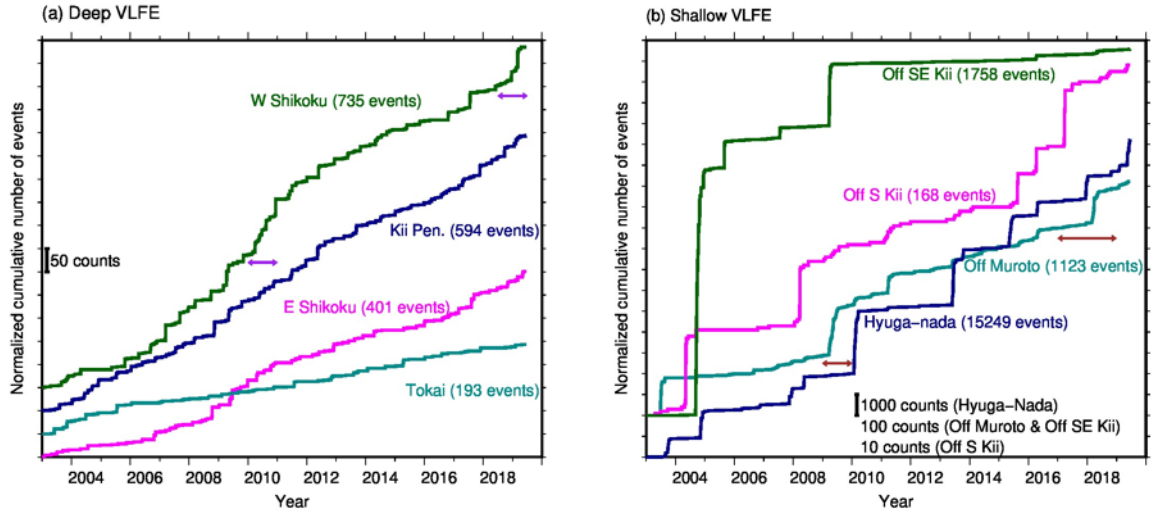
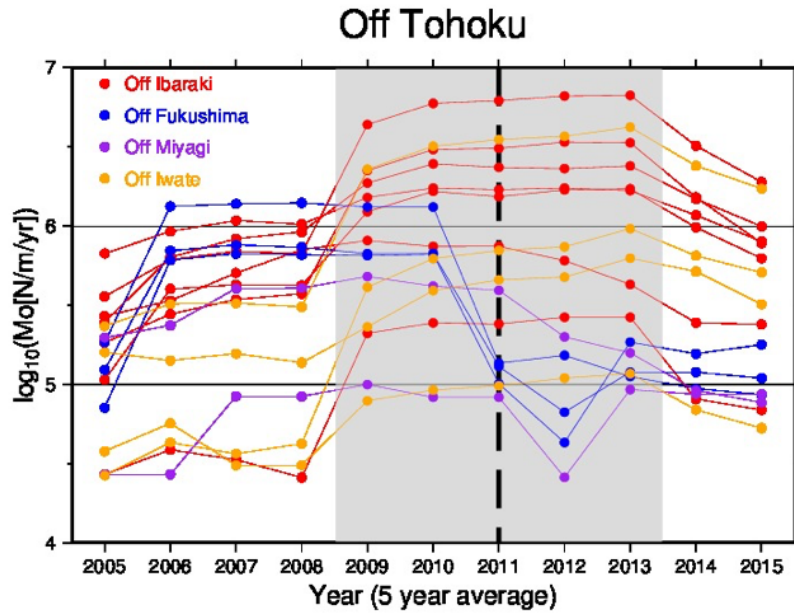


**Figure S4.** Cumulative numbers of events detected from January 2003 to June 2019. (a) Cumulative numbers of deep VLFs. The cumulative number of each group contains events from all virtual epicentral grids in that group. The horizontal purple arrows are the same as those in Figure 2c. (b) Cumulative numbers of shallow VLFs. The cumulative number of each group contains events from all virtual epicentral grids in that group. The horizontal brown arrows are the same as those in Figure 2d.

(a)



(b)

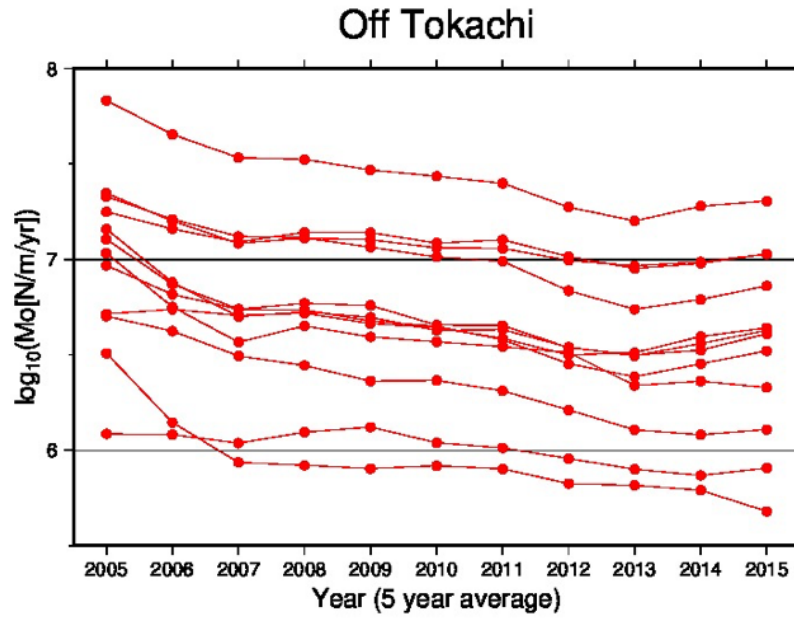


**Figure S5.** Temporal variation of the moment density release rate. (a) Temporal variation of the moment density release rate for each grid based on the 5-year moving average off Tohoku. The black broken line shows the year of the Tohoku earthquake. The period, which includes the year of the Tohoku earthquake based on the 5-year moving average, is filled in grey. (b) Same as (a) but for the region off Tokachi.

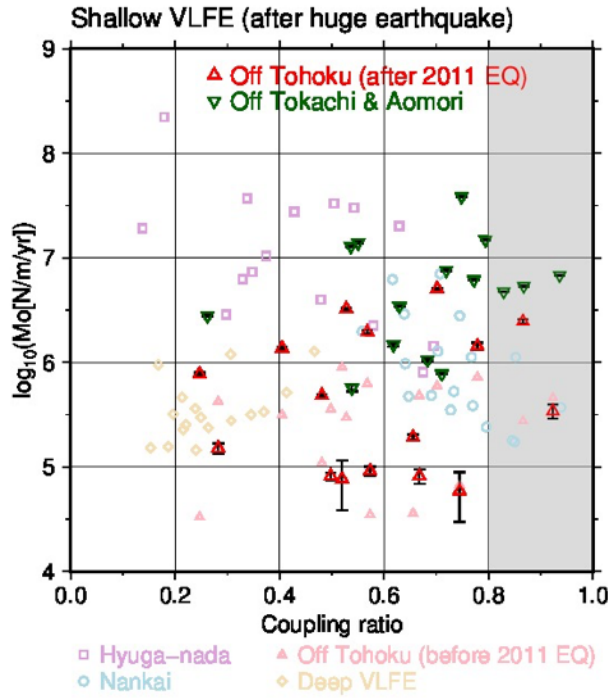


**Figure S6.** Relationship between the moment density release rate after huge earthquakes and interplate coupling ratio. Same as Figure 3 but for shallow VLFs that occurred after huge earthquakes. Light symbols indicate the distribution of deep VLFs and shallow VLFs before huge earthquakes.

**Data Set S1.** List of origin times of detected VLFs. First column: year, second column: month, third column: day, forth column: hour, fifth column: minute, sixth column: second, seventh column: longitude, eighth column: latitude, ninth column: depth, and tenth column: region name. Times are described in JST (UT+9).